Sensorless PMSM Control using Fifth Order EKF in Electric Vehicle Application

Nanda Avianto Wicaksono
Electrical Engineering,
Universitas Indonesia
Kampus UI Depok 16424, West Java, Indonesia
nanda.avianto@esdm.go.id

Bernadeta Wuri Harini
Electrical Engineering,
Universitas Indonesia
Kampus UI Depok 16424, West Java, Indonesia
wuribernard@usd.ac.id

Feri Yusivar
Electrical Engineering,
Universitas Indonesia
Kampus UI Depok 16424, West Java, Indonesia
yusivar@yahoo.com

***Abstract*—This paper is intended to design a controller and an observer of a sensorless PMSM (permanent magnet synchronous motor) in electric vehicle application. The controller uses the field orientation control (FOC) method and the observer type is the fifth order extended Kalman filter (EKF). The designed controller and observer are tested by varying the elevation angle of the route that is several times abruptly changed. The simulation result shows that the designed controller and observer can respond to the elevation angles given.**

Keywords—Sensorless PMSM, FOC, EKF, electric vehicle, elevation angle, torque load

I. INTRODUCTION

The development and utilization of electric vehicles are getting higher along with the increasing awareness of the environmental friendly energy. Consumer users need electric vehicles that can not only be used in the city, but can also be used in the rural and country side. In the rural and country side, one challenge encountered is the ascending route. The elevation angle in the rural and country side is higher than those in the city. The elevation angle in the rural and country side also changes abruptly. Therefore, it takes an electric vehicle that is able to respond to different types of elevation angles.

The elevation angle of an ascending route affects the torque load that is handled by the motor. In combustion vehicle application, the relation between the elevation angle and the torque load was developed by Kamalakkannan [1]. This model can be used in developing the mechanical part of the electric vehicle model.

The motor used is the sensorless PMSM that is equipped with neither the sensor of the rotational speed of the rotor nor the sensor of the rotor/electric angle position [2]. One of them is needed to run PMSM. To obtain the rotational speed of the rotor or the rotor angle position, an EKF observer is used in this design.

The EKF was used in many applications that use sensorless PMSM. The EKF for sensorless PMSM was developed by Zheng et.al [3], Termizi et.al [4], and Walambe et.al [5]. They developed the fourth order EKF that is able to estimate stator currents in dq-axis, rotational speed of rotor, and electric angle position. The fourth order EKF did not estimate torque load. If the torque load changed abruptly, the fourth order EKF could not estimate the rotation speed of rotor and the electric angle position accurately, but it could if the torque load is relatively or slightly constant. Without rotation speed of rotor and electric angle position, field orientation control (FOC) algorithm could not control PMSM. The developed fourth order EKF was only tested by using one shot of torque load in short term of many seconds. It did not ensure the controller and the observer could work in long term continuously.

In order to respond to the elevation angle of the route that changes abruptly, this paper will develop the fifth order EKF. The fifth order EKF is able to estimate stator currents in dq-axis, rotation speed of rotor, electric angle position, and torque load.

The controller and the fifth order EKF is also tested by varying the elevation angle of the route in long term of several hundred seconds. The elevation angle of the route given is several times changed abruptly.

II. ELECTRIC VEHICLE MODEL

The electric vehicle model consists of four parts, i.e. the mechanical part, the PMSM part, the controller part, and the fifth order EKF. The block diagram of the electric vehicle model is shown in Fig. 1.

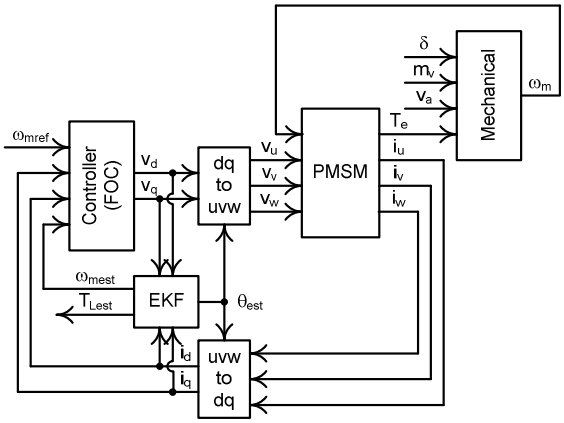

Fig. 1. The electric vehicle model block diagram

A. Mechanical

In an ascending route, there are four forces that work, i.e. inertia force, gradient force, rolling resistance force, and aerodynamic drag force (see Fig. 2)[1].

The inertia force is a force that works when the vehicle accelerates or decelerates. The inertia force is expressed by

$$f_i = m_v a_v = m_v r_w \alpha_w \quad (1)$$

where f_i is the inertia force, m_v is the mass of the vehicle, a_v is the vehicle acceleration/deceleration in translation movement, r_w is the wheel radius, and α_w is the wheel acceleration/deceleration in rotational movement.

The gradient force is a force that works while the vehicle is on an inclined plane. The gradient force is expressed by

$$f_g = m_v g \sin\delta \quad (2)$$

where f_g is the gradient force, m_v is the mass of the vehicle, g is the gravity acceleration, and δ is the elevation angle of the inclined plane.

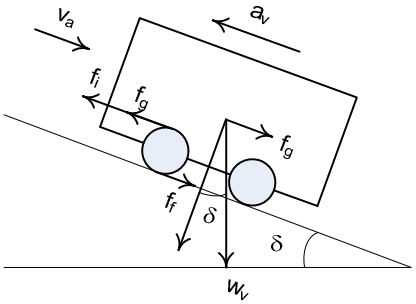

Fig. 2. The electric vehicle on an inclined plane

The rolling resistance force is a friction force between the wheels and the road. The rolling resistance force is expressed by

$$f_f = c_r m_v g \cos\delta \quad (3)$$

where f_f is the rolling resistance force, c_r is the friction coefficient between wheel and road, m_v is the mass of the vehicle, g is the gravity acceleration, and δ is the elevation angle of the inclined plane.

The aerodynamic drag force is a force that works when the vehicle is moving with respect to the surrounding air. The aerodynamic drag force is expressed by

$$f_a = 0.5\,\rho_a c_d A_f (v_v + v_a)^2 \quad (4)$$

where f_a is the aerodynamic drag force, ρ_a is the mass density of air, c_d is the drag coefficient of air, A_f is the front area of the vehicle, v_v is the vehicle velocity, and v_a is the air velocity.

By considering the four forces, the total torque load of the wheel is expressed by

$$T_w = r_w(f_i + f_g + f_f + f_a) \quad (5)$$

where T_w is the total torque load of the wheel and r_w is the wheel radius.

The wheel and the motor are connected by a gear. The gear is the mechanical part that is used to change the speed and the torque between the wheel and the motor. The relation speeds between the wheel and the motor is expressed by

$$\omega_w = \frac{\omega_m}{n_g} \quad (6)$$

where ω_w is the rotational speed of the wheel, ω_m is the rotational speed of the motor, and n_g is the gear ratio.

The relation torques between the wheel and the motor is expressed by

$$\frac{T_w}{\eta n_g} = T_m \quad (7)$$

where T_w is the torque of the wheel, T_m is the torque of the motor, n_g is the gear ratio, and η is the efficiency coefficient of gear.

In rotational movement, the relation between rotational acceleration and torque is are expressed by

$$J_m \frac{d\omega_m}{dt} = T_e - B_m\omega_m - T_{m0} - T_m \quad (8)$$

where J_m is the moment inertia of the motor rotor, ω_m is the rotational speed of the motor, B_m is the friction of the motor, T_{m0} is the initial torque of the motor, and T_m is the total torque load of the motor.

By substitution (1)-(7) to (8) obtains the relation between rotational speed and the torque load of the motor is expressed by

$$\left(J_m + \frac{{r_w}^2 m_v}{\eta {n_g}^2}\right)\frac{d\omega_m}{dt} = T_e - B_m\omega_m - T_{m0} - \frac{r_w}{\eta n_g}(f_g + f_f + f_a) \quad (9)$$

B. PMSM

In this paper, the electrical model of PMSM is expressed by [2]

$$\frac{di_d}{dt} = \frac{-R_s i_d}{L_d} + \frac{N\omega_m L_q i_q}{L_d} + \frac{v_d}{L_d} \quad (10)$$

$$\frac{di_q}{dt} = \frac{-R_s i_d}{L_q} - \frac{N\omega_m L_d i_d}{L_q} - \frac{N\omega_m \psi}{L_q} + \frac{v_q}{L_q} \quad (11)$$

$$T_e = N\psi i_q + NL_d i_d i_q - NL_q i_q i_d \quad (12)$$

$$\frac{d\theta}{dt} = N\omega_m \quad (13)$$

where i_d is the stator current in d-axis, i_q is the stator current in q-axis, v_d is the stator voltage in d-axis, v_q is the stator voltage in q-axis, T_e is the electric torque that is generated by the PMSM, ω_m is the rotational speed of the motor, is the electric angle position, N is number of pole pairs, R_s is the stator resistance, L_d is the inductance in d-axis, L_q is the inductance in q-axis, and ψ is the magnetic flux of the PMSM. The PMSM block diagram is shown in Fig.3.

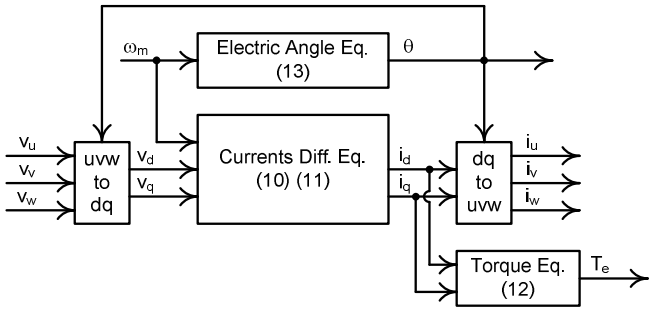

Fig. 3. The PMSM block diagram

C. Controller

The controller part is composed of speed controller, linear current controllers, and nonlinear decoupling references calculation [3]. The controller block diagram is shown in Fig.4.

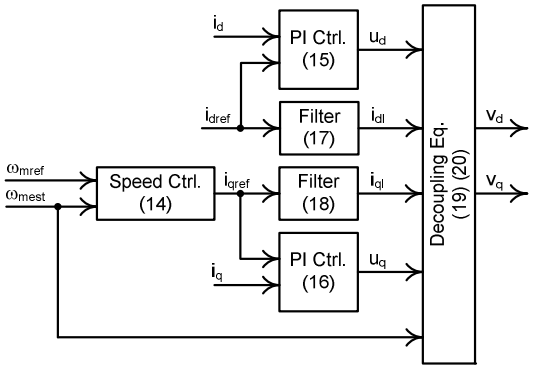

Fig. 4. The controller block diagram

The speed controller uses PI controller. It is expressed by

$$i_{qref} = K_{pw}(\omega_{mref} - \omega_{mest}) + K_{iw}\int_0^t (\omega_{mref} - \omega_{mest})dt \quad (14)$$

where i_{qref} is the reference value of the stator current in q-axis, ω_{mref} is the reference value of the rotational speed of the motor, ω_{mest} is the estimated value of the rotational speed of the motor.

The controller sends the stator voltage references to PMSM. The stator voltage references contained the linear references and the nonlinear references. The linear references are adjusted by two PI controllers that are expressed by

$$u_d = K_{pid}(i_{dref} - i_d) + K_{iid}\int_0^t (i_{dref} - i_d)dt \quad (15)$$

$$u_q = K_{piq}(i_{qref} - i_q) + K_{iiq}\int_0^t (i_{qref} - i_q)dt \quad (16)$$

where u_d is the linear stator voltage references in d-axis, and u_q is the linear stator voltage references in q-axis, i_{dref} is the reference value of the stator current in d-axis i_{qref} is the reference value of the stator current in q-axis, i_d is the actual value of the stator current in d-axis, and i_q is the actual value of the stator current in q-axis. On the other hand, the nonlinear stator voltage references is to consider coupling mechanism in the PMSM.

The total of the stator voltage references are adjusted by two low pass filters and decoupling equations that are expressed by

$$\frac{di_{dl}}{dt} = \frac{1}{T_d}(i_{dref} - i_{dl}) \quad (17)$$

$$\frac{di_{ql}}{dt} = \frac{1}{T_d}(i_{qref} - i_{ql}) \quad (18)$$

$$v_d = u_d - N\omega_{mest}L_q i_{ql} \quad (19)$$

$$v_q = u_q - N\omega_{mest}L_d i_{dl} - N\omega_{mest}\psi \quad (20)$$

where i_{dl} is the low pass filter output of the stator current in d-axis, $i_{ql}$is the low pass filter output of the stator current in q-axis, v_d is the total of the stator voltage references in d-axis, v_q is the total of the stator voltage references in q-axis, u_d is the linear stator voltage references controller in d-axis, u_q is the linear stator voltage references in q-axis, ω_{mest} is the estimated value of the rotational speed of the motor, N is number of pole pairs, L_d is the inductance in d-axis, L_q is the inductance in q-axis, and ψ is the magnetic flux of the PMSM.

D. EKF

In this research, the fifth order EKF is designed to estimate the stator currents in dq-axis, the rotation speed of motor, the electric angle position, and the torque load.

$$x_k = [i_d \quad i_q \quad \omega_m \quad \theta \quad T_L]^T \quad (21)$$

In designing the fifth order EKF, the PMSM model that is used is expressed by

$$\frac{di_d}{dt} = -\frac{R_s i_d}{L_d} + \frac{N\omega_m L_q i_q}{L_d} + \frac{v_d}{L_d} \quad (10)$$

$$\frac{di_q}{dt} = -\frac{R_s i_q}{L_q} - \frac{N\omega_m L_d i_d}{L_q} - \frac{N\omega_m \psi}{L_q} + \frac{v_q}{L_q} \quad (11)$$

$$\frac{d\omega_m}{dt} = \frac{N\psi i_q}{J_m} + \frac{NL_d i_d i_q}{J_m} - \frac{NL_q i_q i_d}{J_m} - \frac{T_L}{J_m} \quad (22)$$

$$\frac{d\theta}{dt} = N\omega_m \quad (13)$$

There are five calculation steps in the algorithm EKF. The five calculation steps are [4,5]

$$\boldsymbol{x}_k^f = \boldsymbol{f}(\boldsymbol{x}_{k-1}^e) \quad (23)$$

$$\boldsymbol{P}_k^f = \boldsymbol{J}_f(\boldsymbol{x}_{k-1}^e)\boldsymbol{P}_{k-1}\left(\boldsymbol{J}_f(\boldsymbol{x}_{k-1}^e)\right)^T + \boldsymbol{Q}_{k-1} \quad (24)$$

$$\boldsymbol{K}_k = \boldsymbol{P}_k^f\left(\boldsymbol{J}_h(\boldsymbol{x}_k^f)\right)^T\left(\boldsymbol{J}_h(\boldsymbol{x}_k^f)\boldsymbol{P}_k^f\left(\boldsymbol{J}_h(\boldsymbol{x}_k^f)\right)^T + \boldsymbol{R}_k\right)^{-1} \quad (25)$$

$$\boldsymbol{x}_k^e = \boldsymbol{x}_k^f + \boldsymbol{K}_k\left(\boldsymbol{z}_k - \boldsymbol{h}(\boldsymbol{x}_k^f)\right) \quad (26)$$

$$\boldsymbol{P}_k = \left(\boldsymbol{I} - \boldsymbol{K}_k\boldsymbol{J}_h(\boldsymbol{x}_k^f)\right)\boldsymbol{P}_k^f \quad (27)$$

III. IMPLEMENTATION AND TEST SCENARIOS

The mathematic model of the electric vehicle is written in the C MEX and simulated by using Matlab/Simulink. The realization of the electric vehicle model is shown in Fig. 5. The parameters of PMSM and mechanical part are listed in Table I and II [6].

TABLE I. PMSM PARAMETERS

Parameters	Quantities	Unit
N	4	pole pairs
ψ	0.08975	V.s/rad
L_d	0.202	mH
L_q	0.29	mH
R_s	8.669	mΩ
J_m	0.01	kg.m^2

TABLE II. MECHANICAL PARAMETERS

Parameters	Quantities	Unit
c_r	0.014	[-]
g	9.81	m.s^{-2}
ρ_a	1.2041	kg.m^{-3}
c_d	0.31	[-]
A_f	2.11	m^2
r_w	0.2933	m
η	0.96	[-]
n_g	12.5	[-]
m_v	900	kg
v_a	2	m.s^{-1}

The electric vehicle model is tested by two test scenarios. Each scenario of the system is done by varying the elevation angle of the route. The first test scenario represents the elevation angle up and down gradually and the second test scenario gives the abrupt changes of the elevation angle of the route.

In the first scenario, the elevation angle given are 0 deg. between 0-50 sec., then 5 deg. between 50-80 sec. and 10 deg. between 80-110 sec., then 15 deg. between 110-140 sec. and 20 deg. between 140-170 sec., then 25 deg. between 170-200 sec. After that, the elevation angle given was 20 deg. between 200-230 sec., then 15 deg. between 230-260 sec. and 10 deg. between 260-290 sec., then 5 deg. between 290-320 sec. and back to 0 deg. between 320-350 sec.(see Fig. 6).

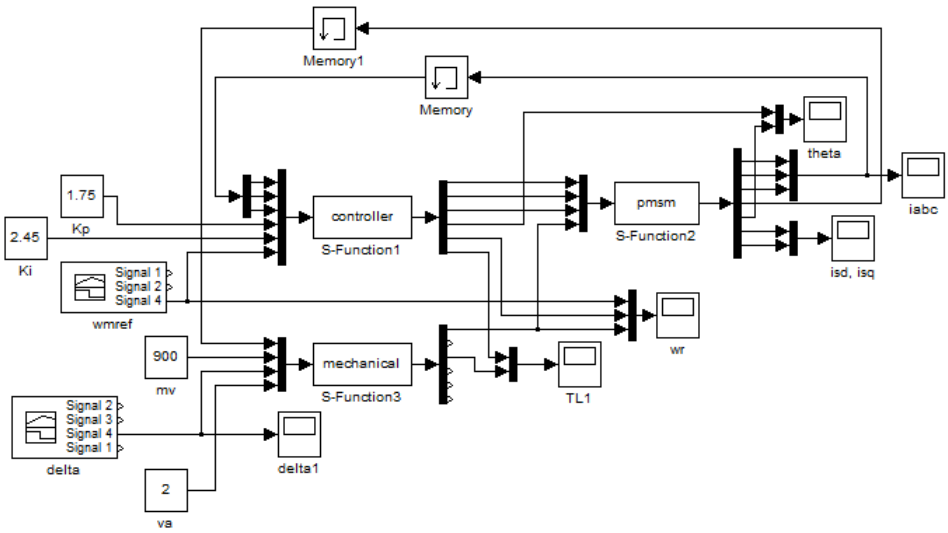

Fig. 5. The implementation of the electric vehicle in Simulink/Matlab

In the second scenario, the elevation angle given are 0 deg. between 0-50 sec., then 22 deg. between 50-80 sec. and back to 0 deg. between 80-110 sec., then 22 deg. between 110-140 sec. and back to 0 deg. between 140-170 sec., then 22 deg. between 170-200 sec, and back to 0 deg. between 170-200 sec., then 22 deg. between 200-230 sec, and back to 0 deg. between 230-250 sec. (see Fig. 7).

In both scenarios, the rotational speed of the motor is kept constantly in 200 rad/s as shown in Fig. 8.

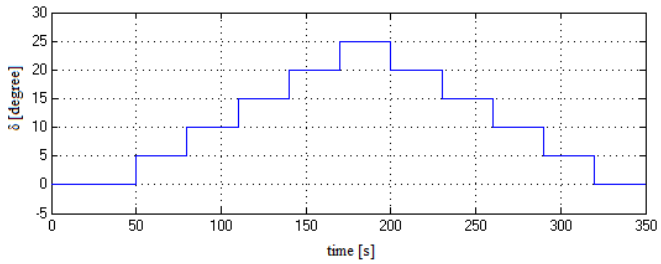

Fig. 6. The elevation angle (δ) in (deg) in the first test scenario

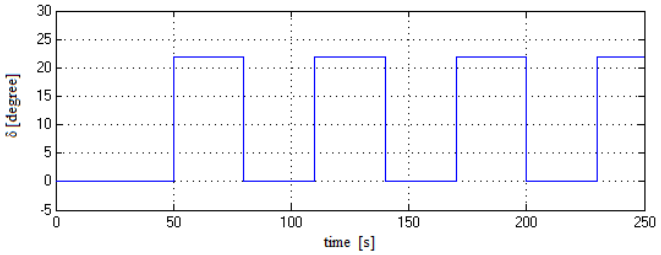

Fig. 7. The elevation angle (δ) in (deg) in the second test scenario

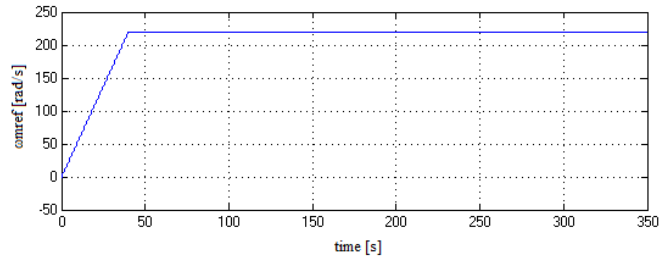

Fig. 8. The speed motor reference

IV. Result and Discuss

The simulation shows that the controller and the fifth order EKF are able to regulate the actual value and the estimated value of the rotational speed of the motor that are close to this reference value.

The additional elevation angle results in the actual value and the estimated value of the rotational speed decrease in the beginning then follow this reference value. On the other hand, the decrease of the elevation angle results in the actual value and the estimated value of the rotational speed increase in the beginning then follow this reference value (see Fig. 9-12).

Fig. 9 and 10 show that the response of the controller and the fifth order EKF in the first test scenario. Fig. 11 and 12 show that the response of the controller and the fifth order EKF in the second test scenario. These results show that the controller and the fifth order EKF can respond to the changes given.

Fig. 10 and 12 show the magnitude changes of the elevation angle influences the over-shoot transient of the actual value and the estimated value of the rotational speed. The 10 deg. magnitude changes influences the over-shoot transient of 15 rad/s (see Fig. 10). The 22 deg. magnitude changes influences the over-shoot transient up to 33 rad/s (see Fig. 12).

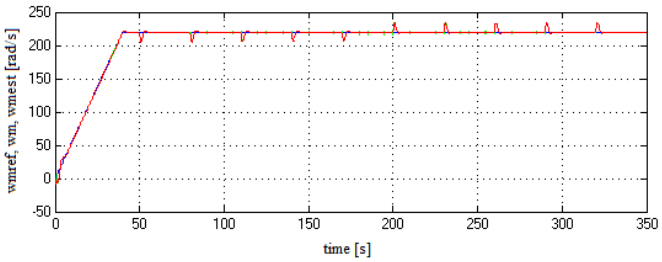

Fig. 9. The reference value (blue), the actual value (red), the estimated value (green) of the rotational speed of the motor in the first test scenario

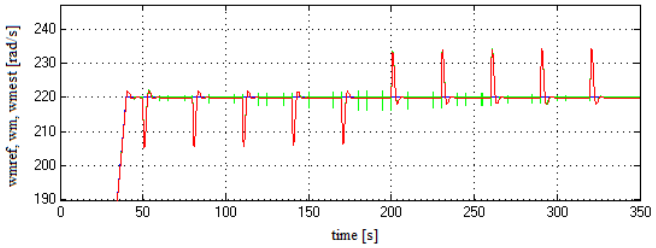

Fig. 10. Zooming the reference value (blue), the actual value (red), the estimated value (green) of the rotational speed of the motor in the first test scenario

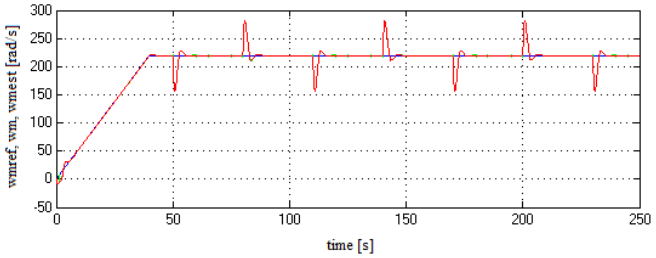

Fig. 11. The reference value (blue), the actual value (red), the estimated value (green) of the rotational speed of the motor in the second test scenario

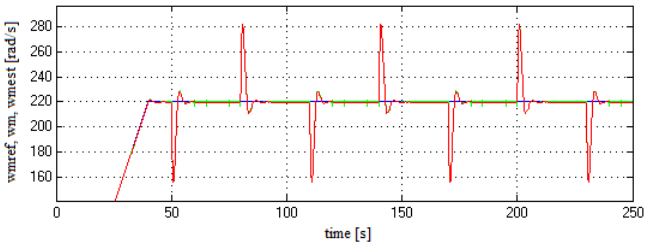

Fig. 12. Zooming the reference value (blue), the actual value (red), the estimated value (green) of the rotational speed of the motor in the second test scenario

Fig. 13 shows the comparison of the actual value (green) and the estimated value (blue) of the electrical angle position in the first test scenario. This result shows the fifth order EKF designed is able to estimate the electric angle position that close to the actual value.

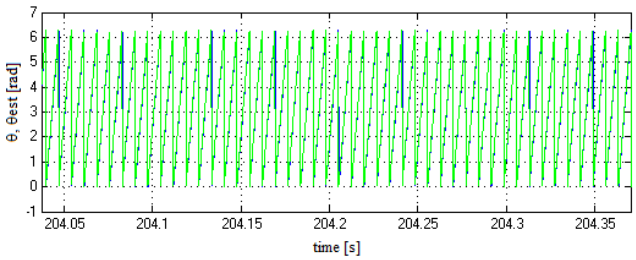

Fig. 13. Comparison of the actual value (green) and the estimated value (blue) of the electrical angle position in the first test scenario

Fig. 14 and 15 show the response of the motor current. The response of the motor current in q-axis follows the changes of the elevation angle. On the other hand, the response of the motor current in d-axis is influenced by nonlinear coupling in PMSM. These results also show the controller and the fifth order EKF can work in the changes given.

Fig. 16 and 17 show the torque load in the mechanical part and the estimated value of the torque load in the fifth order EKF part. The torque load in the mechanical part is represented by green line, and the estimated value of the torque load in the fifth order EKF part is represented by blue line. Both of the torques are able to respond to the changes of the elevation angle that is given in both test scenarios

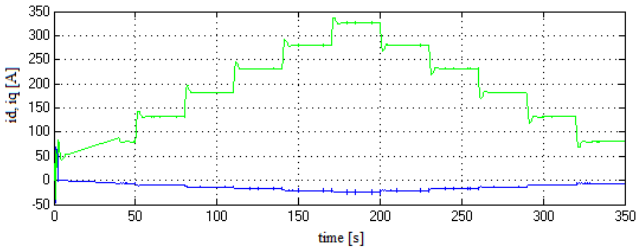

Fig. 14. Motor currents in the first test scenario (id blue, iq green)

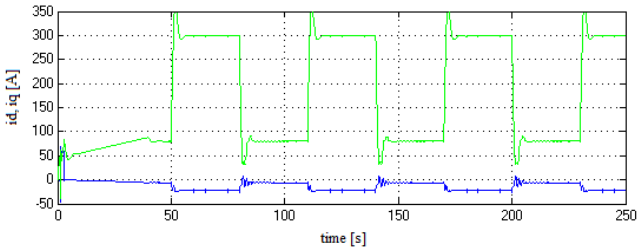

Fig. 15. Motor currents in the second test scenario (id blue, iq green)

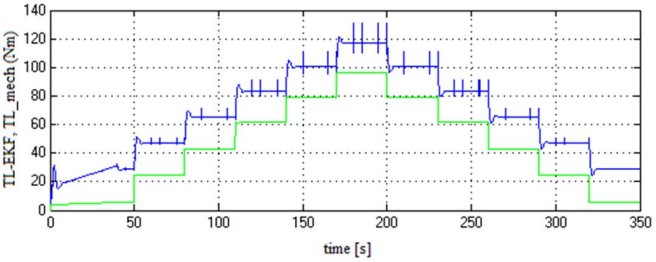

Fig. 16. The estimated value of the torque load in the fifth order EKF part (blue) and the torque load of the mechanical part (green) in the first test scenario

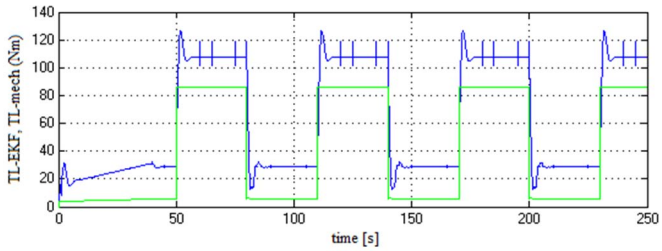

Fig. 17. The estimated value of the torque load in the fifth order EKF part (blue) and the torque load of the mechanical part (green) in the second test scenario

The difference between the torque load in the mechanical part and the estimated value of the torque load in the EKF part is cause by the differences in the definition. The torque load of the mechanical part is expressed by (29).

$$\left(J_m + \frac{{r_w}^2 m_v}{\eta {n_g}^2}\right)\frac{d\omega_m}{dt} = T_e - B_m\omega_m - T_{m0} - T_{L-mech} \quad (28)$$

$$T_{L-mech} = \frac{r_w}{\eta n_g}\left(f_g + f_f + f_a\right) \quad (29)$$

The estimated value of the torque load in the fifth order EKF part is expressed by (31). The result shows the fifth order EKF designed for the PMSM can be used in the electric vehicle model, without changing the model structure of the observer.

$$J_m \frac{d\omega_m}{dt} = T_e - T_{L-EKF} \tag{30}$$

$$T_{L-EKF} = B_m\omega_m + T_{m0} + \frac{{r_w}^2 m_v}{\eta {n_g}^2}\frac{d\omega_m}{dt} + \frac{r_w}{\eta n_g}(f_g + f_f + f_a) \tag{31}$$

V. CONCLUSION

The controller and the fifth order EKF designed are able to regulate the actual value and the estimated value of the rotational speed of the motor in accordance with the reference value. The fifth order EKF is able to estimate the stator currents in dq-axis, the rotation speed of rotor, the electric angle position, and the torque load accurately although the elevation angle of route was changed several times. The result shows the fifth order EKF designed for the PMSM can be used in the electric vehicle model, without changing the model structure of the observer.

ACKNOWLEDGMENT

This research was funded by Universitas Indonesia research grant of the Publikasi Internasional Terindeks untuk Tugas Akhir Mahasiswa (PITTA) UI 2018 No.2439/ UN2.R3.1/HKP.05.00/2018.

REFERENCES

[1] Balaji Kamalakkannan, "Modelling and Simulation of Vehicle Kinematics and Dynamics," Master Thesis, Halmstad University, 2017.

[2] Bernadeta Wuri Harini, Aries Subiantoro, Feri Yusivar, "Stability Analysis of MRAS Speed Sensorless Control of Permanent Magnet Sysnchronous Motor," 2017 International Conference of Sustainable Energy Engineering and Application (ICSEEA), Jakarta, 2017.

[3] Zedong Zheng, Yongdong Li, Maurice Fadel, "Sensorless Control of PMSM Based on Extended Kalman Filter," EPE 2007, Aalborg, 2007.

[4] Mohamad Syakir Termizi, Jurifa Mat Lazi, Zulkifilie Ibrahim, Md Hairul Nizam Talib, M. J. A. Aziz, S. M. Ayob, "Sensorless PMSM drives using Extended Kalman Filter (EKF)," 2017 IEEE Conference on Energy Conversion (CENCON), pp.145 – 150, 2017.

[5] Rahee A. Walambe, Aishwarya A. Apte, Jayawant P. Kolhe, Anjali Deshpande, "Study of Sensorless Control Algorithms for a Permanent Magnet Synchronous Motor Vector Control Drive," 2015 International Conference on Industrial Instrumentation and Control (ICIC), pp.424-428 India, 2015.

[6] Abi Iqbal Prasetyo, "Simulasi Penerapan Motor Listrik Permanen Magnet pada Mobil Listrik Jenis City Car," Bachelor Thesis, Electrical Engineering Universitas Indonesia, 2016.

APPENDIX

$$\boldsymbol{x}_k = [i_d \quad i_q \quad \omega_m \quad \theta \quad T_L]^T \tag{A1}$$

$$f_1 = i_d - \frac{R_s i_d \Delta t}{L_d} + \frac{N\omega_m L_q i_q \Delta t}{L_d} + \frac{v_d \Delta t}{L_d} \tag{A2}$$

$$f_2 = i_q - \frac{R_s i_q \Delta t}{L_q} - \frac{N\omega_m L_d i_d \Delta t}{L_q} - \frac{N\omega_m \psi \Delta t}{L_q} + \frac{v_q \Delta t}{L_q} \tag{A3}$$

$$f_3 = \omega_m + \frac{N\psi i_q \Delta t}{J_m} + \frac{NL_d i_d i_q \Delta t}{J_m} - \frac{NL_q i_q i_d \Delta t}{J_m} - \frac{T_L \Delta t}{J_m} \tag{A4}$$

$$f_4 = \theta + N\omega_m \Delta t \tag{A5}$$

$$f_5 = T_L \tag{A6}$$

$$\boldsymbol{J}_f = \begin{bmatrix} J_{f11} & J_{f12} & J_{f13} & J_{f14} & J_{f15} \\ J_{f21} & J_{f22} & J_{f23} & J_{f24} & J_{f25} \\ J_{f31} & J_{f32} & J_{f33} & J_{f34} & J_{f35} \\ J_{f41} & J_{f42} & J_{f43} & J_{f44} & J_{f45} \\ J_{f51} & J_{f52} & J_{f53} & J_{f54} & J_{f55} \end{bmatrix} \tag{A7}$$

$$J_{f11} = 1 - \frac{R_s \Delta t}{L_d} \tag{A8}$$

$$J_{f12} = \frac{N\omega_m L_q \Delta t}{L_d} \tag{A9}$$

$$J_{f13} = \frac{NL_q i_q \Delta t}{L_d} \tag{A10}$$

$$J_{f14} = 0 \tag{A11}$$

$$J_{f15} = 0 \tag{A12}$$

$$J_{f21} = -\frac{N\omega_m L_d \Delta t}{L_q} \tag{A13}$$

$$J_{f22} = 1 - \frac{R_s \Delta t}{L_q} \tag{A14}$$

$$J_{f23} = -\frac{NL_d i_d \Delta t}{L_q} - \frac{N\psi \Delta t}{L_q} \tag{A15}$$

$$J_{f24} = 0 \tag{A16}$$

$$J_{f25} = 0 \tag{A17}$$

$$J_{f31} = \frac{NL_d i_q \Delta t}{J_m} - \frac{NL_q i_q \Delta t}{J_m} \tag{A18}$$

$$J_{f32} = \frac{N\psi \Delta t}{J_m} + \frac{NL_d i_d \Delta t}{J_m} - \frac{NL_q i_d \Delta t}{J_m} \tag{A19}$$

$$J_{f33} = 1 \tag{A20}$$

$$J_{f34} = 0 \tag{A21}$$

$$J_{f35} = -\frac{\Delta t}{J_m} \tag{A22}$$

$$J_{f41} = 0 \tag{A23}$$

$$J_{f42} = 0 \tag{A24}$$

$$J_{f43} = N\Delta t \tag{A25}$$

$$J_{f44} = 1 \tag{A26}$$

$$J_{f45} = 0 \tag{A27}$$

$$J_{f51} = 0 \tag{A28}$$

$$J_{f52} = 0 \tag{A29}$$

$$J_{f53} = 0 \tag{A30}$$

$$J_{f54} = 0 \tag{A31}$$

$$J_{f55} = 1 \tag{A32}$$

$$\boldsymbol{J}_h = \begin{bmatrix} 1 & 0 & 0 & 0 & 0 \\ 0 & 1 & 0 & 0 & 0 \end{bmatrix} \tag{A33}$$

$$\boldsymbol{Q} = \begin{bmatrix} 2 & 0 & 0 & 0 & 0 \\ 0 & 2 & 0 & 0 & 0 \\ 0 & 0 & 2 & 0 & 0 \\ 0 & 0 & 0 & 2 & 0 \\ 0 & 0 & 0 & 0 & 2 \end{bmatrix} \tag{A34}$$

$$\boldsymbol{R} = \begin{bmatrix} 2 & 0 \\ 0 & 2 \end{bmatrix} \tag{A35}$$